Tests of fundamental symmetries on isolated compound-nucleus resonances

V. E. Bunakov,* E. D. Davis,† and H. A. Weidenmüller
Max-Planck-Institut für Kernphysik, Heidelberg, Federal Republic of Germany
(Received 11 May 1990)

Previous theoretical work has shown that parity and time-reversal symmetry can be tested with particularly high sensitivity in the domain of isolated compound-nucleus resonances. In this domain, experiments will naturally focus on individual resonances rather than on the background cross section. The theoretical analysis of this situation leads to the concept of an ensemble of "on-resonance" measurements. This concept naturally emerges by combining two previous theoretical approaches to tests of fundamental symmetries. We investigate the properties of this new ensemble and show how to convert "on-resonance" data into statistically significant information on symmetry violation.

I. INTRODUCTION

During the last decade it has been established that compound-nucleus (CN) reactions provide particularly sensitive tests for parity and time-reversal symmetry. Experiments[1] on the transmission of polarized neutrons through a ^{139}La target gave a signal for parity violation on the 10% level. This large effect has been qualitatively understood as being due to the combined action of several sizable nuclear enhancement factors. At present, a concerted effort is under way[2] to carry out systematic measurements on parity violation in a number of nuclei. The possibility of extending such measurements to tests of time-reversal symmetry is being investigated.

This experimental work has been accompanied by theoretical investigations. Obvious questions are the following: At which domain of excitation energy and mass number are tests of fundamental symmetries particularly sensitive?[3,4] What is the best choice of observables for such tests? How is a measured symmetry violation (or a bound for such violation) related to the strength of the effective symmetry-breaking nucleon-nucleon interaction?

In this paper, we address tests of fundamental symmetries with polarized neutrons in the domain of isolated CN resonances. Previous work[5,6] comparing the sensitivity of tests of fundamental symmetries in the various CN domains, has shown that this domain is a particularly promising one. In it, there exist two theoretical approaches (briefly sketched in the next two paragraphs) to the problem. It turns out that neither of them as it stands provides the tools necessary to convert experimental information gained from the investigation of isolated resonances into information on the symmetry-breaking part of the Hamiltonian. This situation, briefly explained below, furnishes the motivation for the present work.

One of the approaches[7–9] considers two close-lying CN resonances that are mixed by the symmetry-breaking interaction. In this framework, it is shown that the symmetry-violation effects are strongly enhanced in the vicinity of each resonance by a factor inversely proportional to the resonance width Γ ("resonance enhancement"). Moreover, the "dynamical enhancement" due to the small spacing D between resonances is also seen to be important. The two types of enhancement combine and can yield an enhancement factor 10^6 or so for parity violation, and 10^3 or so for the fivefold correlation test of time-reversal symmetry. (These values apply to neutron transmission with medium-weight and heavy nuclei.) The difficulty inherent in this approach results from the highly complex nature of the wave function of the CN resonances: The experimental determination of a mixing matrix element immediately poses the question of how to relate this piece of data to the underlying symmetry-breaking Hamiltonian. It is well known that, in the CN regime, such a relation can only be of a statistical nature. This then calls for an extension of the approach of Refs. 7–9 to include the stochastic character of CN resonances.

The second approach[5,6] circumvents this difficulty by introducing from the outset a statistical model: The Hamiltonian governing the CN is modeled as an ensemble of random matrices of suitable symmetry, and to this Hamiltonian is added a small piece that breaks the symmetry and is likewise modeled as an ensemble of random matrices.[10–13] It has been possible in this framework to calculate ensemble averages over relevant observables. Such ensemble averages are, via an ergodic theorem, related to energy averages of observables measured on a single realization of the ensemble, i.e., on the atomic nucleus under investigation. To date, only unbiased energy averages have been computed. They must be viewed as a stopgap.[12] The experimental investigation[2] will focus on energies where the symmetry violation is expected to be most strongly enhanced, i.e., on discernible isolated resonances. In the energy regions between resonances, the effect of symmetry violation is expected to be much weaker. Only in the event that the requisite isolated resonances are not identified, will the use of unbiased averages be appropriate.

A proper interpretation of experimental "on-resonance" data obtained in the regime of isolated CN resonances requires the introduction of a biased ensemble. The bias takes account of the fact that data are taken at the location of the resonances. It is the purpose of the present paper to construct this biased ensemble, and to use it in connecting experimental "on-resonance" data

with the symmetry-breaking part of the Hamiltonian.

In Sec. II, we specify precisely the neutron transmission observables we consider, and quote expressions identifying the S-matrix elements to which they are related. In Sec. III, we summarize the first of the two approaches mentioned above, the model of two isolated resonances, for both parity and time-reversal symmetry violation. We point out where statistical concepts must be introduced. The formulas of the two-resonance model (their derivation is contained in an Appendix) are basic to the construction of biased ensembles. In Sec. IV, we present a critique of the statistical approach, and describe an approximate evaluation of unbiased averages which permits a generalization to the case of biased averages. We then introduce the notion of "on-resonance" or biased ensembles. For pedagogical reasons, we proceed in the following steps. We consider first a parity violation involving a two-level and a many-level situation with known resonance parameters (Sec. V). In Sec. VI, we treat the fivefold correlation test of time-reversal symmetry, assuming an admixture of resonances with unknown resonance parameters, and we consider how a confidence limit can be deduced from a set of null data with unknown resonance parameters. Our analytical work in this case is not complete since an exact calculation would require the integration over the full Gaussian orthogonal ensemble (GOE) eigenvalue distribution. We therefore supplement it by a numerical simulation. Section VII contains the conclusions.

II. NEUTRON TRANSMISSION OBSERVABLES FOR SYMMETRY VIOLATIONS

The natural observables are the transmission asymmetries

$$\epsilon=\frac{N_+-N_-}{N_++N_-}\ . \tag{1}$$

Here N is the number of transmitted neutrons. In parity-violation studies with polarized neutrons and unpolarized targets (the configuration employed to date), the indices $\pm$ designate the incident neutron helicity. For the fivefold correlation, the indices $\pm$ denote the incident neutron polarization parallel-antiparallel to $\mathbf{k}\times\mathbf{c}$, $\mathbf{k}$ being the beam wave vector and $\mathbf{c}$ a unit vector along the direction of the "crystal" axis of the spin-aligned target. Under conditions of good energy resolution, ϵ is simply related to the difference $\Delta\sigma=(\sigma_+-\sigma_-)/2$ in the total cross sections $\sigma_\pm$:

$$\epsilon=-nz\Delta\sigma\ , \tag{2}$$

where n is the atomic number density of the target and z its thickness. In turn, via the optical theorem, $\Delta\sigma$ is linear in *elastic* S-matrix elements.

We restrict ourselves to neutrons of kinetic energy $E\lesssim 100$ eV. We also consider measurements performed at a particular p-wave resonance of angular momentum J (the significance of such measurements is discussed in Sec. III). Then, for parity-violation studies (with polarized neutrons and an unpolarized target),

$$\Delta\sigma=\frac{2\pi}{k^2}\rho\frac{(2J+1)}{(2I+1)}\mathrm{Re}[S_J(0\tfrac{1}{2};1\tfrac{1}{2})]\ , \tag{3}$$

where I is the target spin and the elastic S-matrix elements $S_J(lj;l'j')$ are with respect to a j-coupled basis [the full coupling scheme is $((l,\frac{1}{2})j,I)J$]. In terms of statistical tensors $t_{KQ}(s)$ (Madison convention), the beam-polarization parameters $\rho=t_{1/2\,0}(\frac{1}{2})$.[14] The parity-violating character of $\Delta\sigma$ in Eq. (3) is apparent from the difference in relative orbital angular-momentum quantum numbers $\Delta l=l'-l=1$. Measurements with polarized targets and unpolarized neutrons are complicated by the fact that $\Delta\sigma$ depends on both $S_J(0\frac{1}{2};1\frac{1}{2})$ and $S_J(0\frac{1}{2};1\frac{3}{2})$.

The corresponding expression in the case of the fivefold correlation involves the antisymmetrized elastic S matrix $S^{(a)}$, with elements

$$S_J^{(a)}(lj;l'j')=\tfrac{1}{2}[S_J(lj;l'j')-S_J(l'j';lj)]\ . \tag{4}$$

There are two kinematically equivalent contributions to $\Delta\sigma$: a pp term $\Delta\sigma_{pp}$ and an sd term $\Delta\sigma_{sd}$. (The labeling refers to the elastic neutron partial waves involved.) As we treat, by way of illustration, measurements performed at a particular p-wave resonance (of angular momentum J),

$$\Delta\sigma\approx\Delta\sigma_{pp}=\frac{2\pi}{k^2}\rho'\frac{3}{\sqrt{5}}\frac{\sqrt{J+1/2}}{(2I+1)}f\ \mathrm{Im}[S_J^{(a)}(1\tfrac{1}{2};1\tfrac{3}{2})]\ , \tag{5}$$

where $f=-\sqrt{2I-1}$ $(+\sqrt{2I+3})$ for $J=I+\frac{1}{2}(I-\frac{1}{2})$, and, in terms of statistical tensors $\hat{t}_{KQ}(s)$ referring to the beam and target symmetry axes, the polarization parameter $\rho'=\hat{t}_{10}(\frac{1}{2})\hat{t}_{20}(I)$.[14]

In subsequent sections, we use the abbreviated notation S_P and S_T to denote the S-matrix elements in Eqs. (3) and (5), respectively.

III. OPTIMAL CONDITIONS: THE MODEL OF TWO ISOLATED RESONANCES

We summarize the findings on the optimal conditions (in the isolated resonance regime) for neutron transmission studies of parity and time-reversal violation

A. Parity violation

In the simplified case of a single s-wave and single p-wave resonance, the main contribution to $\mathrm{Re}(S_P)$ in Eq. (3) is given by

$$\mathrm{Re}(S_P)\cong-\tfrac{1}{2}\gamma_n^s\gamma_{n\ 1/2}^p\times\frac{(E-E_s)\Gamma_p+(E-E_p)\Gamma_s}{[(E-E_s)^2+\frac{1}{4}\Gamma_s^2][(E-E_p)^2+\frac{1}{4}\Gamma_p^2]}v_P\ . \tag{6}$$

Here, $\Gamma_{s,p}$ are the total widths and $E_{s,p}$ the energies of the resonances, E is the energy of the neutron, and v_P is the weak-interaction matrix element connecting the two resonant states; $\gamma_{n\ 1/2}^p$ is one of the (real-valued) partial neutron width amplitudes γ_{nj}^p of the p-wave resonance,

and γ_n^s is the partial neutron width amplitude of the s-wave resonance. For simplicity, we shall take $\Gamma_s \cong \Gamma \cong \Gamma_p$. (We recall that the total width stems mainly from the decay into gamma channels.)

The presence of the two Breit-Wigner denominators leads, for $E \cong E_{s,p}$, to an enhancement of $\mathrm{Re}(S_P)$ in the vicinity of *either* resonance by a factor $(D/\Gamma)^2$, with $D = E_s - E_p$. This is the "resonance enhancement" factor. It reflects the fact that parity mixing increases with the time $\hbar/\Gamma$ spent by the neutron within the region of the weak interaction. When the practical consideration of the choice of target thickness necessary to minimize statistical counting errors for a given incident neutron flux is taken into account (the relevant quantity is the ratio $\Delta\sigma/\sigma_{\mathrm{tot}}$), it is seen that the resonance enhancement survives *only* for measurements in the vicinity of the p-wave resonance.[8]

Resonance enhancement increases with decreasing width to spacing ratio of the resonances. This last fact suggests that the enhancement is particularly pronounced near neutron threshold and for nuclei where the resonant states are highly complex configurations. In this situation, there is no way of calculating the matrix element v_P from a nuclear model, and to deduce the strength α_P of the parity-violating interaction from a comparison of the calculated value with the data. The only way to obtain information on α_P is via a statistical approach. This approach has shown its validity in the analysis of spectral fluctuation properties of CN resonances.

From the statistical point of view, the ensemble of matrix elements v_P connecting the p-wave resonances in a given nucleus with their neighboring s-wave resonances of the same angular momentum J is a sample drawn from a Gaussian distribution with mean value zero. The variance $\langle v_P^2 \rangle$ (where $\langle\ \rangle$ denotes a running average over matrix elements in a given nucleus) is the only meaningful piece of information relating to the strength α_P. [From the theoretical point of view (discussed more extensively in Sec. IV), it is preferable to introduce a fictitious ensemble of nuclear Hamiltonians. Then, each matrix element between an s-wave and a p-wave resonance is a Gaussian random variable in its own right. Matrix elements between different s-wave and $p$wave pairs are uncorrelated, but all have the same variance $\overline{v_P^2}$, which coincides with the running average $\langle v_P^2 \rangle$.]

Adopting the statistical point of view, we observe that, in the CN regime, the admixture parameter v_P/D is much bigger than it would be for standard parity experiments which involve pairs of simple configurations of nuclear states of opposite parity and with typical spacings of 100 keV or so. Therefore, the small spacing of CN resonances leads to further enhancement. To quantify this statement, we introduce the spreading width (with d denoting the mean-level spacing of states of a given parity and angular momentum J)

$$\Gamma_P^{\downarrow} \equiv 2\pi \langle v_P^2 \rangle / d \tag{7}$$

of the parity-violating interaction and use the fact that $\Gamma_P^{\downarrow}$, as any spreading width, is expected to depend very little on excitation energy and/or mass number. This implies that $\langle v_P^2 \rangle^{1/2}/d$ $[\sim(\Gamma_P^{\downarrow}/d)^{1/2}]$ increases like $d^{-1/2}$ with decreasing spacing between the nuclear states. Comparing a typical parity-violation experiment in a light nucleus ($d \cong 100$ keV) with the CN experiment ($d \cong 10$ eV), we obtain an enhancement ("dynamical enhancement") which is at least of the order of $[(100\ \mathrm{keV}/(10\mathrm{eV})]^{1/2} \cong 10^2$. Other approaches to this problem lead to even bigger estimates of the enhancement.

The expression (6) is a gross simplification of the actual situation and hides a problem of the present approach: A given p-wave resonance will mix not only with the closest, but with all nearby s-wave resonances. As a consequence, the expression (6) for $\mathrm{Re}(S_P)$ should contain a sum over several or many s-wave resonances and, therefore, a number of matrix elements of the parity-violating Hamiltonian (rather than a single matrix element). From the measurement of parity violation on a given p-wave resonance, it is impossible to deduce the values of all these matrix elements. This observation accentuates the need for an alternative (statistical) treatment.

B. Time-reversal violation

The simplest model involves the mixing (under a time-reversal-odd–parity-even interaction V_T) of two p-wave resonances, labeled 0 and 1, respectively. Paralleling Eq. (6),

$$\mathrm{Im}(S_T) \cong -\tfrac{1}{2}(\gamma_{n\,1/2}^{p_0}\gamma_{n\,3/2}^{p_1} - \gamma_{n\,1/2}^{p_1}\gamma_{n\,3/2}^{p_0}) \times \frac{(E-E_0)\Gamma_1 + (E-E_1)\Gamma_0}{[(E-E_0)^2 + \frac{1}{4}\Gamma_0^2][(E-E_1)^2 + \frac{1}{4}\Gamma_1^2]} v_T\ , \tag{8}$$

where $v_T = \mathrm{Im}[(V_T)_{01}]$, $(V_T)_{01}$ being the matrix element of V_T between the two resonant states 0 and 1. As in Sec. III A, $\mathrm{Im}(S_T)$ shows resonance enhancement in the vicinity of *either* p-wave resonance. Violation of time-reversal symmetry is also dynamically enhanced in the CN regime.[7] We note that, for targets of optimal thickness ($\approx$ two mean free paths), it is advantageous[7] to look for strong p-wave resonances ($\sigma_p \cong \sigma_{\mathrm{tot}}$); by contrast, in the case of parity violation, the optimal situation occurs[8] when $\sigma_s \sim \sigma_p > \sigma_{\mathrm{pot}}$. [Here, σ_s (σ_p) denotes the contribution (ignoring interference terms) to the total cross section σ_{tot} from the s- (p-) wave resonance under consideration.]

The arguments presented under Sec. III A show that a statistical extension of the above treatment is again necessary. We must characterize V_T by its spreading width

$$\Gamma_T^{\downarrow} \equiv 2\pi \langle v_T^2 \rangle / d\ . \tag{9}$$

The interaction V_T will mix a given p-wave resonance with *all* p-wave resonances (of the same angular momentum) in its vicinity; this fact calls for an extension of Eq. (8) to a many-level formula. There is a further difficulty: whereas, for s-wave resonances, energies, total and partial neutron amplitudes are usually known, this is not so for

p-wave resonances. We address this problem in Sec. VI.

A case has also been made[14] for measurements at very weak s-wave resonances ($\sigma_s \ll \sigma_{\rm tot} \approx \sigma_{\rm pot}$). These can, in principle, display similar enhancements, because of the admixture under V_T of the d-wave components of adjacent s-wave resonances. We shall not pursue measurements of this type: their treatment parallels that of Sec. VI.

Finally, experiments on time-reversal violation are expected to yield upper bounds rather than actual values. Further statistical arguments are needed to convert such upper bounds into bounds on the spreading width $\Gamma_T^{\downarrow}$.

IV. SYMMETRY BREAKING IN THE STATISTICAL MODEL: NO BIASING

The difficulties which arise in the two-level model of Sec. III are completely avoided in the statistical approach.

A. Critique

The essential ingredient concerns the treatment of the Hamiltonian

$$H = H^{(0)} + H^{(1)} , \tag{10}$$

where $H^{(0)}$ preserves and $H^{(1)}$ breaks the symmetry under consideration. The symmetry-conserving $H^{(0)}$ is modeled as an ensemble of random matrices (of the GOE type for time-reversal symmetry breaking; as a reducible matrix with two diagonal sub-blocks of the GOE type for parity violation to simulate the two classes of opposite parity). The symmetry-breaking perturbation is likewise modeled as an ensemble of matrices with uncorrelated Gaussian distributed random variables as matrix elements. Through an ergodic theorem, the average of an observable (expressed as a functional of H) over the H ensemble is equated with the running average (i.e., the energy average) over a single member of the ensemble, i.e., the CN under consideration.

As regards neutron transmission studies, these random matrix models have, to date, been applied to the rigorous calculation, for both parity violation and fivefold correlation, of the unbiased variance of $\Delta\sigma$, $(\Delta\sigma)^2$. The treatment is rigorous in the sense that the variances are exact to leading nonvanishing order in the small perturbation $H^{(1)}$ and they apply in the entire CN regime, from the regime of isolated resonances to the regime of Ericson fluctuations. By unbiased, we mean that the variances are to be equated with energy averages inferred from measurements of $\Delta\sigma$ at several *arbitrary* energies in the regime of interest. It is averages of this type which are most accessible to rigorous theoretical treatment.

Results for the unbiased variances $\overline{(\Delta\sigma)^2}$ serve one important function: they allow one to investigate the utility of poor energy-resolution measurements in the isolated resonance regime (at present, unavoidable for polarized neutrons in the keV range), or of neutron transmission studies at higher energies (beyond the isolated resonance regime), where $\Delta\sigma$ is no longer kinematically suppressed. However, our focus in this paper is in that portion of the domain of isolated resonances (neutron energies $E < 100$ eV) where good-resolution high-statistics experiments are currently being attempted. Here, unbiased variances must be viewed as a stopgap, appropriate only if the conditions for measurement discussed in Sec. III cannot be realized. Recall that the main contribution to $\Delta\sigma$ comes from energies close to resonance, while, in the remaining vast energy interval between resonances, the contributions are $(d/\Gamma)^2$ times smaller. Thus, to determine the unbiased $\overline{(\Delta\sigma)^2}$, experimental groups would be confronted with a painstaking and not very promising search for symmetry violation in resonance-free regions. (There is also the problem that transmission experiments at or near s-wave resonances are bound to suffer from poor statistics.) Therefore, experimental investigations should naturally focus on isolated p-wave resonances (where possible).

B. Approximate evaluation of $\overline{(\Delta\sigma)^2}$ (isolated resonance regime)

The discussion above shows that it is necessary to formulate and work out a statistical approach which takes account from the outset of the natural bias introduced experimentally. As preparation, it is helpful to review the derivation of the unbiased variances $\overline{(\Delta\sigma)^2}$ within an approximate scheme tailored to the isolated resonance regime (in the limit of many open channels). We consider the case of the fivefold correlation, for which the unbiased estimate, because of experimental constraints, may be of interest in its own right: ^{165}Ho is, at present, the only feasible target, and there are no known p-wave resonances in ^{166}Ho for neutron energies below 100 eV. (This is not the case for parity-violation studies: there are several targets to choose from with known p-wave resonances.)

We start from the many-level generalization of Eq. (8):

$$\mathrm{Im}(S_T) = -\tfrac{1}{2} \sum_{i<k} (\gamma_{n\,1/2}^{p_i}\gamma_{n\,3/2}^{p_k} - \gamma_{n\,1/2}^{p_k}\gamma_{n\,3/2}^{p_i}) \frac{(E-E_i)\Gamma_k + (E-E_k)\Gamma_i}{[(E-E_i)^2+\frac{1}{4}\Gamma_i^2][(E-E_k)^2+\frac{1}{4}\Gamma_k^2]} (v_T)_{ik} . \tag{11}$$

According to the statistical model, the partial-width amplitudes $\gamma_{nj}^{p_k}$ are uncorrelated Gaussian random variables with zero mean values and (k- independent) second moments equal to the average partial width $\overline{\Gamma_{nj}^{p}}$. Likewise, the matrix elements $(v_T)_{ik}$ are uncorrelated Gaussian random variables of zero mean and common variance $(d/2\pi)\Gamma_T^{\downarrow}$. The total widths Γ_i obey a χ^2 distribution with ν degress of freedom, where ν is the number of open channels.[15] We take $\nu \gg 1$ (justified by the large number of gamma channels), so that the distribution is almost a delta function and $\Gamma_i \cong \Gamma$ for all i. The resonance energies E_i (identified with GOE eigenenergies) are further random variables, not correlated with the partial amplitudes, total widths, and matrix elements of V_T. There-

fore, the variance of $\mathrm{Im}(S_T)$ is given by

$$\overline{[Im(S_T)]^2}=\frac{1}{2}\frac{2\pi\overline{\Gamma^9_{n\,1/2}}}{d}\frac{2\pi\overline{\Gamma^p_{n\,3/2}}}{d}g\frac{2\pi\Gamma^{\downarrow}_T}{d}\ , \tag{12}$$

where the average over the GOE eigenvalue distribution is confined to

$$g=t^2\left[\frac{d}{2\pi}\right]^6 \times\sum_{i<k}\frac{(2E-E_i-E_k)^2}{[(E-E_i)^2+\frac{1}{4}\Gamma^2]^2[(E-E_k)^2+\frac{1}{4}\Gamma^2]^2}\ , \tag{13}$$

with $t\equiv 2\pi\Gamma/d$. Note that, in keeping with the ensemble concept discussed earlier, the average is performed at fixed energy E.

The reduction of g is standard. Rescaling the resonance energies by their mean separation d, g can be expressed in terms of a two-dimensional integral (over $x_i=E_i/d$ and $x_k=E_k/d$) with the two-level correlation function $R_2(x_i,x_k)$ (Ref. 16) as weight. In the limit of physical interest, namely $N\to\infty$ (N is the number of GOE eigenstates),

$$R_2(x_i,x_k)\to 1-Y_2(|x_i-x_k|)$$

(Ref. 16) so that, transforming to integration variables $q=x_i+x_k$ and $r=x_i-x_k$, and performing the integral over q, we find

$$g=\frac{1}{\pi^2 t}\int_0^\infty dr[1-Y_2(r)]\frac{1}{r^2+(t/2\pi)^2} \equiv\frac{1}{t^2}\Phi_0(t/2\pi)\ , \tag{14}$$

a notation first used by Moldauer.[17] Further simplification is possible after substituting for the two-level cluster function Y_2 in terms of its Fourier transform: $\Phi_0(z/\pi)$ can be compactly expressed as

$$\Phi_0(z/\pi)=1-\frac{1}{z}+\frac{e^{-z}}{z^2}\sinh z +\frac{1}{z}\left[\cosh z-\frac{1}{z}\sinh z\right][-\mathrm{Ei}(-z)]\ . \tag{15}$$

(Ei is the exponential integral.) We note that, for $t\ll 1$,

$$g\approx\frac{1}{6t}(\alpha_0-\ln t)\ , \tag{16}$$

where $\alpha_0=2+\ln 2-\zeta\approx 2.12$ (ζ is Euler's constant) and terms of order t^2 and higher have been dropped.

A treatment of this kind can be extended to the case of on-resonance measurements by identifying the energy E above with the energy of the resonance E_0 at which the measurement is performed. Averages like that in Eq. (13) then become averages over "on-resonance" ensembles, which can be evaluated using the statistical distributions introduced above. The procedure will be acceptable provided it is ergodic (in the sense of Ref. 18): the ensemble average of an observable is equal to the running average of the same observable taken over a set of nuclear states.

V. "ON-RESONANCE" ENSEMBLES: PARITY

In Secs. III and IV we have demonstrated the necessity to approach the analysis of data obtained in the investigation of symmetry violations in a novel way. In the present section, we construct ensembles which suit this purpose for parity violation. For pedagogical reasons, we proceed in steps, starting with the two-level model of Sec. III.

A. Parity violation in the two-level model

We consider the model of Sec. III A, use Eq. (6) at $E=E_p$, and assume that positions, partial-width amplitudes, and total widths of the two resonances are known. Then,

$$\mathrm{Re}(S_P)_{E=E_p}\equiv\mathrm{Re}(S_P)_p\cong\frac{\gamma^p_{n\,1/2}}{\Gamma_p}\frac{\gamma^{\backslash}_n}{E_s-E_p}v_P \equiv A_p v_P \tag{17}$$

is the product of a known constant A_p and the parity-violating matrix element v_p. The behavior of v_P for different choices of resonance pairs can be modeled (within an ensemble formulation) by supposing that it is a Gaussian random variable with variance $(v_P)^2=\Gamma^{\downarrow}_P d/2\pi$. This suggests that we could introduce an "on-resonance" ensemble by considering $\mathrm{Re}(S_P)_p$ as a Gaussian random variable with zero mean value, and a variance $[\mathrm{Re}(S_P)_p]^2=A_p^2\overline{v_P^2}$. Doing so, however, would not be correct, for the following reason. The introduction of an ensemble, in the context of nuclear physics, makes sense only if there is reason to believe that ergodicity applies, i.e., the ensemble average of an observable is equal to the running average of the same observable taken over a set of nuclear states, because obviously only the latter average can be realized experimentally. For $\mathrm{Re}(S_P)_p$ to be ergodic, it is necessary that $\mathrm{Re}(S_P)_p$ be independent of the resonances actually investigated. But this is not the case because the factor A_p will change with the actual pair of resonances considered. A meaningful ensemble is obtained by considering

$$\Delta_P(p)=\mathrm{Re}(S_P)_p/A_p\ . \tag{18}$$

This variable is ergodic. In the present trivial example, $\Delta_P(p)$ coincides with v_P, but this is not so in general (cf. Sec. V B). The example serves to illustrate the general point that attention must be given to the definition of appropriate *ergodic* variables.

We also use this simple case to indicate how $\Gamma^{\downarrow}_P$ (or an upper bound on this quantity) can be deduced from a set of m measurements, taken on p-wave resonances labeled $i=1,\ldots,m$ with resonance parameters A_i. To this end, we consider a variant of the additive noise model of Ref. 19.

Let $\Delta_P(i)$ denote the ergodic random variable of Eq. (18) at the ith resonance. We recall that in the framework of our theoretical model, Δ_P has a Gaussian probability distribution; the value $\Delta_P(i)$ at the ith resonance is drawn from this distribution. A measurement of Δ_P at

the ith resonance will introduce an additional probabilistic element: at each resonance, the experiment yields a probability distribution rather than a precise value for the observable; details of this distribution will depend on the actual experiment. Assuming that there are no systematic errors, and that the quantities N_i in Eq. (1) are sufficiently large compared to unity, it is possible to argue that the experimental distribution is approximately Gaussian at each resonance, with a mean value given by $\Delta_P(i)$ and a width related to the experimental error $\delta\Delta_P(i)$. Assuming the Gaussians at all resonances to have the same width, we conclude that the probability distribution of the measured observable Δ_P^{expt} is obtained by folding the theoretical distribution [in the present case a Gaussian, but, in, for example, the case considered in Sec. VI, the function P_a of Eq. (43)] with the Gaussian describing the experimental distribution. In the present case, this yields a Gaussian with zero mean value and a second moment given by $\overline{\Delta_P^2}+\sigma^2$, where σ^2 is the width of the experimental Gaussian distribution. This form then lends itself to a maximum-likelihood analysis, in which the m measured values $\Delta_P(i)$ and the m experimental errors $\delta\Delta_P(i)$ are substituted for the argument of the Gaussian and the quantity σ, respectively. With obvious modifications, this procedure also serves to establish upper bounds in the case of time-reversal symmetry breaking.

This is an additive noise model because an equivalent formulation says that Δ_P^{expt} is the sum of the theoretical random variable Δ_P and an uncorrelated noise term $\delta\Delta_P$; the latter has a Gaussian probability distribution centered at zero with variance σ^2.

B. Parity violation in a more realistic model

We consider first the extension to accommodate the admixture of a number of s-wave resonances, and then the modifications when the p-wave partial-width amplitude is unknown (relevant to the use of spin-nonzero targets).

1. Many levels

The model of Sec. V A is unrealistic because it stipulates that the parity-violating interaction admixes only the closest s-wave resonance into the given p-wave resonance. A more realistic model consists in allowing for the admixture of a number of s-wave resonances. In this case, $\mathrm{Re}(S_P)$ takes the form (we put $E=E_p$)

$$\mathrm{Re}(S_P)_p \cong 2\frac{\gamma^p_{n\,1/2}}{\Gamma_p}\sum_k \frac{\gamma^{s_k}_n}{E_{s_k}-E_p}(v_P)_k = \sum_k A_{pk}(v_P)_k \ . \tag{19}$$

The index k labels the s-wave resonances. Under the assumption that the parameters of all s resonances are known, $\mathrm{Re}(S_P)_p$ is a sum of Gaussian distributed random variables $(v_P)_k$ with constant coefficients and therefore itself a Gaussian. However, as in Sec. V A, $\mathrm{Re}(S_P)_p$ is not ergodic. We therefore define

$$\Delta_P(p)\equiv\frac{\mathrm{Re}(S_P)_p}{\left[\sum_k A_{pk}^2\right]^{1/2}} \ . \tag{20}$$

The variance of $\Delta_P(p)$ (any p) is given by $\overline{v_P^2}$ [all $(v_P)_k$ have the same variance as required by ergodicity] showing that $\Delta_P(p)$ is ergodic. Given a set of values $\Delta_P(i)$ or of upper bounds B_i on $\Delta_P(i)$ from measurements on a set of p-wave resonances $i=1,\ldots,m$, the analysis now proceeds as in Sec. V A.

2. Unknown p-wave partial-width amplitudes

In the case of the two-resonance model, we would now write $\mathrm{Re}(S_P)_p$ as [cf. Eq. (17)]

$$\mathrm{Re}(S_P)_p \cong B_p\gamma^p_{n\,1/2}v_P \ , \tag{21}$$

the product of a known constant B_p, the p-wave partial-width amplitude $\gamma^p_{n\,1/2}$ and the parity-violating matrix element v_P. Like v_P, the behavior of the unknown $\gamma^p_{n\,1/2}$ for different choices of resonance pairs can be modeled (within an ensemble formulation) by supposing that it is a Gaussian random variable of zero mean; the variance is $\overline{\Gamma^p_{n\,1/2}}$, which is simply related to a neutron strength function. The p-wave partial-width amplitude $\gamma^p_{n\,1/2}$ and the parity-violating matrix element v_P are independent random variables. Thus, we introduce an on-resonance ensemble by considering

$$\hat{\Delta}_P(p)=\mathrm{Re}(S_P)_p/B_p \ , \tag{22}$$

which [like $\Delta_P(p)$] is ergodic and has probability density

$$\frac{1}{\pi\omega}K_0[\hat{\Delta}_P(p)/\omega] \ . \tag{23}$$

Here, K_0 is MacDonald's function of zero order and $\omega^2=\overline{\Gamma^p_{n\,1/2}(v_P)^2}$ is the variance of $\hat{\Delta}_P(p)$. [We have appealed to the fact that, if z is the product of two independent Gaussian random variables of zero mean and unit variance, then it has probability density $K_0(z)/\pi$.]

In the many-level generalization, we write [cf. (19)]

$$\mathrm{Re}(S_P)_p \cong \gamma^p_{n\,1/2}\sum_k B_{pk}(v_P)_k \ , \tag{24}$$

and define

$$\hat{\Delta}_P(p)\equiv\frac{\mathrm{Re}(S_P)_p}{\left[\sum_k B_{pk}^2\right]} \ . \tag{25}$$

VI. "ON-RESONANCE" ENSEMBLES: FIVEFOLD CORRELATION

A much more complex situation than that considered in Sec. V arises when the resonance parameters of the resonances which are admixed into a given resonance, are unknown. This case is likely to arise with the fivefold correlation test of time-reversal symmetry. Indeed, the time-reversal violating interaction mixes p-wave resonances with each other, and p-wave resonance parameters

are poorly known in general. In this case, we have to resort to a purely statistical description, taking for the resonance parameters the distribution predicted by the GOE.

A. Time-reversal violation in a many-level model

We consider a measurement performed at a p-wave resonance 0. In the many-level case, the dominant contribution to $\mathrm{Im}(S_T)$ at $E=E_0$ is given by [cf. Eqs. (8) and (11)]

$$\mathrm{Im}(S_T)_0 \cong \frac{2}{\Gamma_0}\sum_{k\neq 0}(\gamma^{p_0}_{n\,1/2}\gamma^{p_k}_{n\,3/2}-\gamma^{p_0}_{n\,3/2}\gamma^{p_k}_{n\,1/2}) \times \frac{E_{p_k}-E_0}{(E_{p_k}-E_0)^2+\frac{1}{4}\Gamma^2_{p_k}}(v_T)_k \ . \tag{26}$$

The index k labels the admixed p-wave resonances. We assume the neutron partial widths $\Gamma^{p_0}_{n\,1/2}$ and $\Gamma^{p_0}_{n\,3/2}$ to be known. As regards the remaining resonance parameters, we adopt the statistical description outlined in Sec. IV B. In particular, this means that we set all Γ_{p_k}'s including Γ_0 equal to Γ. Then, an ergodic equilvalent of equivalent of $\mathrm{Im}(S_T)_0$ is [cf. Eq. (20)]

$$\Delta_T = \mathrm{Im}(S_T)_0/(\Gamma^{p_0}_{n\,1/2}\overline{\Gamma^{p}_{n\,3/2}}+\Gamma^{p_0}_{n\,3/2}\overline{\Gamma^{p}_{n\,1/2}})^{1/2} \ . \tag{27}$$

Proceeding as in the derivation of Eq. (12), we find for the variance of Δ_T

$$\overline{\Delta^2_T} \cong \left[\frac{2}{\Gamma}\right]^2 g_{\text{biased}}\frac{\overline{v^2_T}}{d^2} \ , \tag{28}$$

where

$$g_{\text{biased}} = \sum_k \frac{d^2(E_0-E_{p_k})^2}{[(E_0-E_{p_k})^2+\frac{1}{4}\Gamma^2]^2} \ . \tag{29}$$

The calculation of g_{biased} resembles that of g in Eq. (12). We find

$$g_{\text{biased}} = 2\int_0^\infty dr[1-Y_2(r)]\frac{r^2}{\{r^2+[t/(4\pi)]^2\}^2} \ , \tag{30}$$

or, in terms of Φ_0,

$$g_{\text{biased}} = \frac{2\pi^2}{t}\left[\Phi_0\left(\frac{t}{4\pi}\right)+\frac{t}{4\pi}\Phi_0'\left(\frac{t}{4\pi}\right)\right] \ , \tag{31}$$

where Φ_0' denotes the derivative of Φ_0 with respect to its argument. Combining these results, we obtain, for $t \ll 1$,

$$\overline{\Delta^2_T} \cong \frac{1}{3\Gamma^2}(2.31-\ln t)\frac{2\pi\Gamma^{\downarrow}_T}{d} \ . \tag{32}$$

It is of interest to compare the result (32), or rather $\overline{\Gamma^{p}_{n\,1/2}\Gamma^{p}_{n\,3/2}\Delta^2_T}$ with the unbiased energy average of Sec. IV B. When $t \ll 1$, the two factors (in brackets) containing $\ln t$ are approximately equal. So, we find that $\overline{\Gamma^{p}_{n\,1/2}\Gamma^{p}_{n\,3/2}\Delta^2_T}$ is bigger than the unbiased average by a factor $\simeq 4/t$. By selecting only "on-resonance" points for our statistical ensemble, we enhance the effect expected on average by a resonance enhancement factor $\sim d/\Gamma$. This clearly shows the advantage of using the "on-resonance" ensemble.

B. Upper bound on time-reversal violation

The result derived in Sec. VI A is useful only if nonvanishing values for Δ_T have been measured. Actually we expect that only upper bounds on $|\Delta_T|$ are available. In such a case, one would wish to proceed as in Sec. V A: To use the distribution function of the ergodic observable corresponding to Δ_T to obtain a bound on $\Gamma^{\downarrow}_T$. In the present case, the distribution function is not Gaussian, and we proceed to derive an approximation P_a to its form from the defining equations.

We use Eq. (26), put $\Gamma_k=\Gamma$ for all k, introduce the dimensionless random variables

$$x_k = \frac{(v_T)_k}{[\overline{v^2_T}]^{1/2}} \ ,$$

$$y_k = \frac{\gamma^{p_0}_{n\,1/2}\gamma^{p_k}_{n+3/2}-\gamma^{p_0}_{n\,3/2}\gamma^{p_k}_{n\,1/2}}{(\Gamma^{p_0}_{n\,1/2}\overline{\Gamma^{p}_{n\,3/2}}+\Gamma^{p_0}_{n\,3/2}\overline{\Gamma^{p}_{n\,1/2}})^{1/2}} \ , \tag{33}$$

$$c_k = \frac{(E_0-E_k)d}{(E_0-E_k)^2+\frac{1}{4}\Gamma^2} \ ,$$

and observe that the x_k and y_k are uncorrelated Gaussian variables with zero mean and unit variance, and that the distribution of the c_k is determined by the GOE eigenvalue distribution $P(E_0,E_1,E_2,\ldots)$, with E_0 kept fixed.

Instead of Δ_T, we consider the dimensionless ergodic random variable

$$\delta_T = \sum_{k\neq 0} x_k y_k c_k \ . \tag{34}$$

The normalized probability density $P(\delta_T)$ is given by

$$P(\delta_T) = \int dE_1 dE_2 \cdots P(E_0,E_1,E_2,\ldots) \times \prod_{j\neq 0}\left[\frac{1}{\sqrt{2\pi}}\int dx_j \exp(-\tfrac{1}{2}x_j^2)\right] \times \prod_{k\neq 0}\left[\frac{1}{\sqrt{2\pi}}\int dy_k \exp(-\tfrac{1}{2}y_k^2)\right] \times \delta\left[\delta_T - \sum_l x_l y_l c_l\right] \ . \tag{35}$$

We write the delta function as a Fourier integral over ω and carry out the integrations over the y_k and over ω. After the substitution $x_j \to c_j x_j$, this yields

$$P(\delta_T) = \int dE_1 dE_2 \cdots P(E_0,E_1,E_2,\ldots) \times \prod_{j\neq 0}\left[\frac{1}{(2\pi c_j^2)^{1/2}}\int dx_j \exp\left[-\frac{1}{2}\frac{x_j^2}{c_j^2}\right]\right] \times \frac{1}{(2\pi\sum_{k\neq 0}x_k^2)^{1/2}}\exp\left[-\frac{1}{2}\frac{\delta_T^2}{\sum_{k\neq 0}x_k^2}\right] \ . \tag{36}$$

It is instructive to discuss the form (36). The last factor, taken by itself with all the x_j fixed, would yield a Gaussian for $P(\delta_T)$. However, the x_j themselves are Gaussian random variables. If all the c_j were fixed and roughly equal, $\sum_{k\neq 0} x_k^2$ would be proportional to a χ^2- distributed quantity with a large number of degrees of freedom, and hence would—to a very good degree of approximation—be given by $\sum_j c_j^2$, resulting again in a Gaussian distribution for $P(\delta_T)$ with variance $\sum_j c_j^2$. However, the c_j^2 are neither fixed nor equal. Indeed, Eq. (33) shows that with $E_1, E_2, \ldots$ arranged in such a way that

$$|E_0-E_1| \leq |E_0-E_2| \leq |E_0-E_3| \leq \ldots ,$$

the c_j^2 decrease rapidly with increasing j. Moreover, c_1^2 has fluctuations which are large compared to those of c_2^2 and so on. For these reasons, we circumvent the exact integration over $P(E_0,E_1,E_2,\ldots)$ in Eq. (36) (which we cannot perform) by the following approximation. With E_1 denoting the eigenvalue closest to E_0, we divide the domain of integration over E_1 into two parts, given by $|E_1-E_0| > -\varepsilon d$ and by $|E_1-E_0| < \varepsilon d$, respectively. Here, $\varepsilon \gg \Gamma/d$ has a value ($\varepsilon \simeq \frac{1}{2}$ or so, ε will be fully specified below) such that for $|E_1-E_0| \geq \varepsilon d$ many terms in the sum Eq. (34) have approximately equal weight (so that δ_T is Gaussian), while for $|E_1-E_0| < \varepsilon d$ the $j=1$ term in Eq. (34) dominates the rest.

For $|E_1-E_0| \geq \varepsilon d$, we accordingly replace the right-hand side of Eq. (36) by a Gaussian. The variance is approximately given by using a picket-fence model for the eigenvalues, yielding $\sum_j c_j^2 \simeq \pi^2/3$. This contribution to $P(\delta_T)$ accordingly has the form

$$\frac{\sqrt{3}}{\pi\sqrt{2\pi}} p \exp[-3\delta_T^2/2\pi^2] . \tag{37}$$

The weight factor p with $0<p<1$ is determined below.

For the remaining integration over E_1 with $|E_0-E_1| < \varepsilon d$, we use a picket-fence model for all E_k's except the eigenvalues closest to E_0, yielding

$$\sum_{j\neq 1} c_j^2 \simeq \pi^2/3 - 1 = \alpha ,$$

and carry out the remaining integration over $|E_1-E_0| = sd$, using the (normalized) Wigner surmise. As a result, we find, with

$$c_1 = c(s) \equiv s/(s^2+\Gamma^2/4d^2) ,$$

$$2\left[\frac{\pi}{2}\int_0^{\varepsilon} ds\, s \exp\left[-\frac{\pi}{4}s^2\right]\right]\left[\frac{1}{(2\pi c^2)^{1/2}}\int_{-\infty}^{\infty} dx \exp\left[-\frac{x^2}{2c^2}\right]\right]\left\{\frac{1}{[2\pi(x^2+\alpha)]^{1/2}}\exp\left[-\frac{\delta_T^2}{2(x^2+\alpha)}\right]\right\} . \tag{38}$$

The factor 2 arises because E_1-E_0 can have either sign.

The approximate probability density function $P_a(\delta_T)$ is given by the sum of the contributions in Eqs. (37) and (38). The normalization condition yields

$$p = 2\exp\left[-\frac{\pi}{4}\varepsilon^2\right] - 1 . \tag{39}$$

The calculation of the second moment gives, for $\Gamma/d \ll 1$,

$$\overline{\delta_T^2} = \frac{\pi^2}{3} + \pi\ln 2 + \pi\ln\varepsilon - 2\left[1-\exp\left[-\frac{\pi}{4}\varepsilon^2\right]\right]$$

$$-\frac{\pi}{2}\left\{1+\int_0^{(\pi/4)\varepsilon^2} dw \frac{[1-\exp(-w)]}{w}\right\} - \pi\ln\frac{\Gamma}{d} . \tag{40}$$

In comparing this with the result implied by Eq. (32),

$$\overline{\delta_T^2} = \frac{\pi^2}{3}\left[2.31 - \ln 2\pi - \ln\frac{\Gamma}{d}\right] , \tag{41}$$

we first note that the dependence on Γ/d is nearly the same: the difference, i.e., the factor $\pi/3$ is due to the different behavior of $1-Y_2(r)$ and of the Wigner surmise for small values of the argument. The constants in Eqs. (40) and (41) cannot be quite matched for $\varepsilon \simeq \frac{1}{2}$, the value in Eq. (40) being smaller than that in Eq. (41) by $\simeq 0.5$. We do not aim at a better agreement, as this would involve fixing α, which seems irrelevant in view of the rough approximations used above.

Higher moments of δ_T are, for $\Gamma \ll d$, dominated entirely by negative powers of Γ/d; these originate from the small s behavior of the integrals in Eq. (38). We find, for $n>1$ and $\Gamma \ll d$,

$$\overline{\delta_T^{2n}} \cong \frac{\pi}{2}\frac{[(2n-1)!!]^2}{(n-1)}\left[\frac{\Gamma}{2d}\right]^{2-2n} . \tag{42}$$

We observe that the result in Eq. (42) is independent of α which again shows that for $n>1$, the moments $\overline{\delta_T^{2n}}$ are essentially determined by the resonances closest to E_0. We note that the calculation leading to Eq. (42) is the better, the larger n is, since the high moments of δ_T are most strongly dominated by the large-δ_T behavior of $P_a(\delta_T)$ or, equivalently, by the small-s behavior of $c(s)$. Comparison with the numerical results will show that the low moments are not terribly well given by Eq. (42).

Returning to the approximate probability density $P_a(\delta_T)$, we are led to write it in the form

$$P_a(\delta_T)=p\frac{\sqrt{3}}{\pi\sqrt{2\pi}}\exp[-3\delta_T^2/(2\pi^2)]+\int_0^{\epsilon}ds(s^2+\Gamma^2/4d^2)\exp\left[-\frac{\pi}{4}s^2\right]$$
$$\times\int_0^{\infty}dx\frac{1}{[x^2+\alpha]^{1/2}}\exp\left[-\frac{\delta_T^2}{2(x^2+\alpha)}-\frac{x^2}{2c^2(s)}\right]. \quad (43)$$

In Appendix B, we indicate the essential differences of an alternative treatment, appropriate when the restriction that both neutron partial widths $\Gamma_{nj}^{p_0}$ be known, is dropped. We note that, under the assumption that

$$\overline{\Gamma_{n\,1/2}^{p}}\approx\tfrac{1}{2}\overline{\Gamma_n^p}\approx\overline{\Gamma_{n\,3/2}^{p}},$$

the above analysis can be employed when only the sum

$$\Gamma_n^{p_0}=\Gamma_{n\,1/2}^{p_0}+\Gamma_{n\,3/2}^{p_0}$$

is known.

C. Comparison with numerical simulations

Our numerical simulations start from the relations defining δ_T, Eqs. (33) and (34). To generate the nontrivial component $\{c_j\}$, we adopt the following conceptually simple procedure: we draw Hamiltonian matrices of a fixed dimension N from the corresponding GOE, diagonalize numerically, and form the required eigenvalue differences (E_0 is identified with the eigenvalue nearest the center of the spectrum to minimize effects associated with the finiteness of N), scaled by the theoretically known average level spacing at the center of the spectrum. If these differences are denoted by z_j ($j=1,\ldots,N-1$), then we set

$$c_j=\frac{z_j}{z_j^2+(t/4\pi)^2}, \quad (44)$$

where the constant $t/2\pi$ is the value of Γ/d assumed. In what follows, simulation data will be represented in the form of binned frequency distributions: if N_i (i is an integer) denotes the number of occurrences in a sample of values of δ_T such that

$$(i-\tfrac{1}{2}b)\le\delta_T<(i+\tfrac{1}{2})b$$

(b is the bin size), then we plot $P_i=N_i/N_{\rm tot}$ vs $(\delta_T)_i=bi$, $N_{\rm tot}$ being the total number of events in the sample. Error bars are assigned under the assumption that the distribution of N_i (i fixed) for different samples is Poissonian.

As regards the choice of N, we are, in principle, interested in the character of the δ_T distribution in the limit $N\to\infty$. Figure 1 is a representative example of our findings concerning the approach to this limit: in it, we compare simulation data for $N=30$ and 60 ($t=0.01$). Note that in this and other diagrams in this subsection, the vertical axis is magnified by a factor of 10. Already the changes with increasing N are sufficiently small for one to be able to argue that, with the present sample sizes, there is no statistically significant difference between the two frequency distributions. If we make the reasonable assumption that increasing the sample sizes will only serve to reduce the error bars, it is possible to discern that the $N=60$ frequency distribution is slightly smaller than the $N=30$ distribution for $\delta_T<1$. Presumably the tail of the $N=60$ data (not displayed) is correspondingly enhanced over that of the $N=30$ data. However, it is precisely the tail region which is least accessible with the present simulation: here, we have to rely on analytic estimates. In the small-δ_T regime, it will be sufficient if the approximate probability distributions we introduce overestimate the magnitude of $P(\delta_T)$. We conclude that, for our purposes, we can take N as small as ~ 30.

Known moments of the δ_T distribution provide obvious checks of the numerical simulation. In all cases, we have confirmed that the distributions inferred from our finite samples have odd moments consistent with zero, and variances consistent with the prediction of Eq. (32). We note that estimators for higher moments are poorly determined whenever $t<0.1$. To cite an example: for $t=0.01$, the statistical error in the estimate for the fourth moment with a sample of 1 000 000, is of the order of 15%. (By contrast, for the same simulation data, the statistical error in the estimate for the variance is of the or-

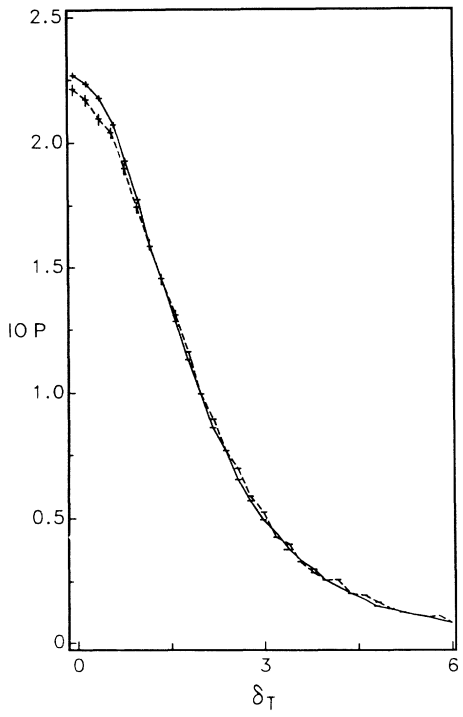

FIG. 1. N dependence of binned frequency distributions inferred from simulation data ($t=10^{-2}$, bin size $b=0.2$). Unbroken line: $N=30$ (sample size $\Sigma=10^6$). Dashed line: $N=60$ ($\Sigma=3\times10^5$). (Error bars included.)

der of a percent.) The problem is exacerbated for smaller values of t. A related observation is that the estimates are not robust. Clearly, these deficiencies of the simulation data arise because of the significance for higher moments of the tail of the distribution, which is poorly determined. We see that the extent of the tail must increase with decreasing t [direct analytic evidence for this is furnished in Eq. (51) below], which we can interpret as a consequence of resonance enhancement. It is also apparent that a frequency distribution inferred from our simulation data has, by itself, limited information content. It should, in principle, be possible to reproduce any such frequency distribution with dissimilar analytical forms that predict essentially the same low-order moments, but wildly different higher-order moments. Hence, the approach (favored by some statisticians) of trying to fit the observed distribution to one of Pearson's family of distributions or another popular class of distributions, is inappropriate.

A comparison of the physically motivated approximate distribution P_a of Eq. (43) with simulation data is presented in Fig. 2. Like the simulation data, P_a has been subjected to a binning procedure. The smooth curve joins discrete points $[(\delta_T)_i,(P_a)_i]$, where

$$(P_a)_i=\frac{1}{b}\int_{(i-1/2)b}^{(i+1/2)b} dx\, P_a(x)\ . \tag{45}$$

In Fig. 2(a), the values of α and ε recommended in Sec. VI A ($\alpha=\pi^2/3-1$ and $\varepsilon=\frac{1}{2}$) have been adopted. In addition, the magnitudes (after binning) of the Gaussian contribution P_g to P_a and the remainder $P_r=P_a-P_g$, are depicted. Figure 2(b) displays the sensitivity to different choices of ε and α. The various features of Fig. 2 illustrate the validity of the assertions of Sec. VI B. We note that, consistent with the discussion following Eq. (42), there is (a) the remarkably good description of the simulation data by P_a in the "wings" of the distribution (intermediate values of δ_T), (b) the deteriorating agreement for small δ_T, and (c) the insensitivity to α ($\alpha\sim 1$) in the wings. In line with the approach take in Sec. VI B, we have not attempted to fine tune the values of α and ε. In fact, it can be seen from Fig. 2(b) that choosing values different from those specified in Sec. VI B will not lead to any significant improvement in the region where P_a is expected to do well.

An interesting perspective on these results is given by an alternative attempt at describing the δ_T frequency distribution. It employs the δ_T distribution when only one resonance contributes to the sum in Eq. (34). Replacing $P(E_0,E_1,\ldots)$ in Eq. (35) by the Winger surmise, the corresponding probability density is

$$p_1(\delta_T)=\tfrac{1}{2}\int_0^\infty ds\, s\,(s^2+\Gamma^2/4d^2)K_0(\delta_T/c(s))\times\exp\left[-\frac{\pi}{4}s^2\right]\ . \tag{46}$$

As a crude alternative to the approximation scheme of Sec. VI B, we can choose to write δ_T as the sum

$$\delta_T=(\delta_T)_{\rm NN}+(\delta_T)_g\ , \tag{47}$$

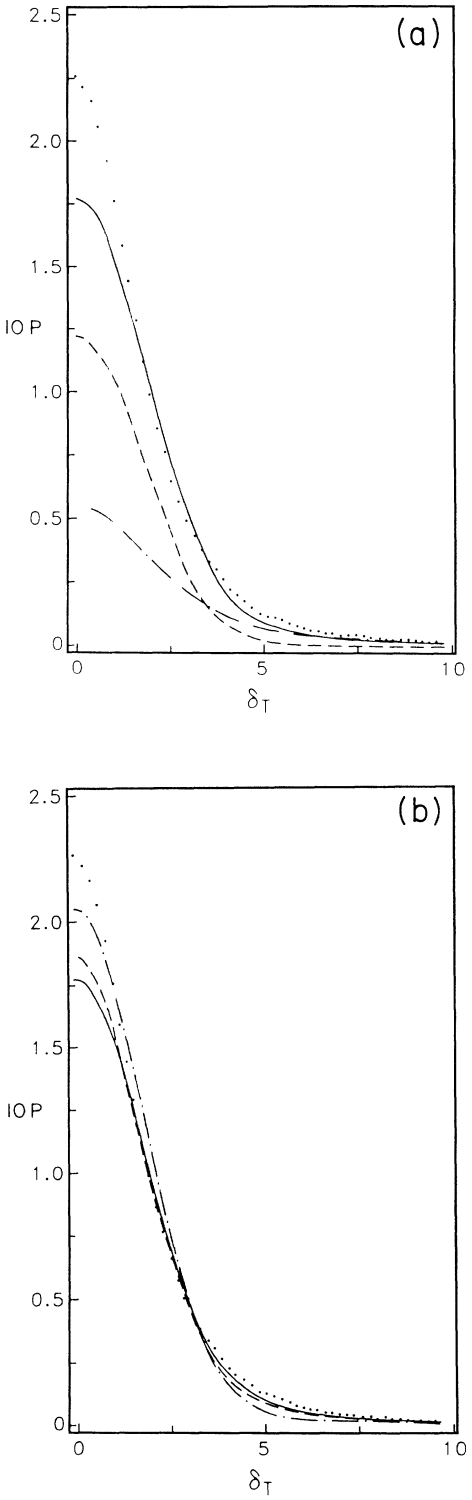

FIG. 2. Comparison of P_a [Eq. (43)] after binning with frequency distribution from simulation data ($N=30$, $\Sigma=10^6$)—$t=10^{-2}$, $b=0.2$. The dots denote the simulation data points. (a) Comparison for $\alpha=\pi^2/3-1$ and $\varepsilon=\frac{1}{2}$. Unbroken line: P_a. Dashed line: P_g. Dot-dashed line: P_r. (b) Sensitivity of P_a to different α and ε. Unbroken line: α and ε as in Fig. 2(a). Dashed line: $\alpha=\pi^2/3-2$ and $\varepsilon=\frac{1}{2}$. Dot-dashed line: $\alpha=\pi^2/3-2$ and $\varepsilon=\frac{1}{4}$.

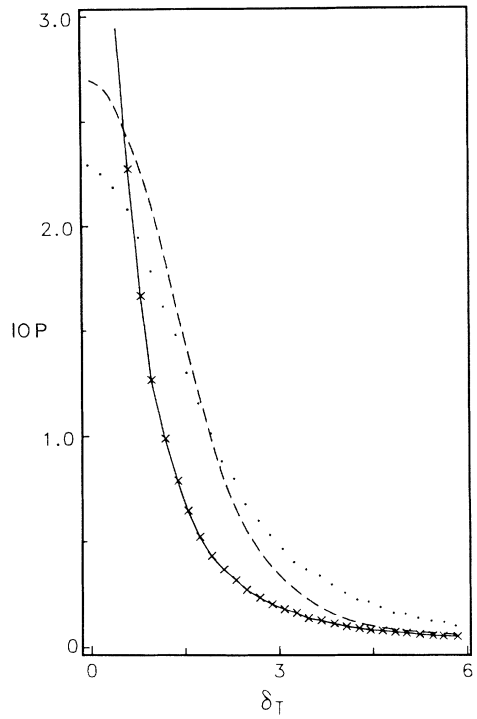

FIG. 3. Comparison of P_c [Eq. (48)] after binning with frequency distribution from simulation data ($N=30$, $\Sigma=10^6$)—$t=10^{-2}$, $b=0.2$. Dots denote the simulation data. Dashed line: P_c. Plots of p_1 [Eq. (46)] are included. Unbroken line: $t=0$. Crosses: $t=10^{-2}$.

where the "nearest-neighbor" contribution $(\delta_T)_{\rm NN}$ is distributed according to Eq. (46) and $(\delta_T)_g$ is a Gaussian random variable of zero mean and variance $\alpha_c^2=\pi^2/3-1$. The associated probability distribution is

$$P_c(\delta_T)=\frac{1}{\sqrt{2\pi}\alpha_c}\int dz\,\exp\left[-\frac{(\delta_T-z)^2}{2\alpha_c^2}\right]p_1(z)\ . \tag{48}$$

In Fig. 3, we compare P_c (after binning) with the simulation data of Fig. 2; also included are plots of p_1 for $t=0$ and 0.01 (no binning). We draw attention to two features. First, P_c underpredicts the simulation data in the wings, a region where P_a is in good agreement. As, for large δ_T, P_c is unambiguously related to $(\delta_T)_{\rm NN}$, this is evidence of the continuing importance of contributions to δ_T from more distant resonances. Here we have a concrete illustration of a shortcoming of the two-resonance model of Sec. III. The second feature concerns the behavior of p_1 for small δ_T. When $t=0$, p_1 can be expressed in terms of a confluent hypergeometric function of the second kind,

$$p_1(z)=\frac{1}{4\sqrt{\pi}}\Psi(\tfrac{3}{2},1;z^2/\pi)\ , \tag{49}$$

from which we infer that p_i diverges as $-\ln\delta_T$ for $\delta_T\to 0$. A hint of this singular behavior can be seen in Fig. 3, which also indicates that a sharp increase in p_1 as $\delta_T\to 0$ persists for nonzero t (<0.1). The additive Gaussian component $(\delta_T)_g$ in Eq. (47) "smears" away this trend (as one would expect), but not enough, as P_c overpredicts the magnitude of $P(\delta_T)$ for small δ_T. The fact that P_a is an underprediction for small δ_T suggests that P_r (in P_a) accommodates too much smearing.

So far, we have not addressed the issue of the t dependence of the δ_T distribution. Again, the example of p_1 is instructive. Recall that p_1 describes the "nearest-neighbor" contribution to δ_T, and hence that component in δ_T which is most sensitive to t. From numerical comparisons like that in Fig. 3, we find that, for small to intermediate values of δ_T, p_1 is insensitive to the precise value of t provided $t<0.1$. However, it is in the tail of p_1 that differences in the magnitude of t are significant: elementary asymptotic analysis yields

$$p_1(z)\sim\frac{\pi}{4}\frac{1}{z^3} \tag{50}$$

when $t=0$, as opposed to

$$p_1(z)\sim\frac{\pi}{2z}\left[\frac{t}{4\pi}\right]^2\exp\left[-\frac{1}{4\pi}(t/4)^2-\frac{t}{2\pi}z\right] \tag{51}$$

when $t>0$.

VII. CONCLUSIONS

In this paper, we have addressed the question of how can information on the strength of the symmetry-breaking part of the Hamiltonian be deduced from tests performed on isolated CN resonances? We have set out from a critique of the model of pairs of isolated resonances and of ensemble averaging. The model of pairs of isolated resonances fails to take into account the effect of more distant resonances, and the fact that resonance parameters, in general, and the symmetry-breaking mixing matrix elements, in particular, are stochastic. The theoretical approach based on (standard) ensemble averaging, on the other hand, fails to account for the bias introduced by investigating isolated resonances, and the enhancement of symmetry breaking that comes with it.

We have avoided the shortcomings of both these approaches by developing a statistical theory of biased ensembles. In doing so, we have emphasized the need to study *ergodic* observables. Depending on the amount of information available on the resonances contributing to the reaction, our theory takes different forms. The most complex situation which we have considered in detail arises when many p-wave resonances with unknown resonance parameters are admixed by the T-violating interaction to a given p-wave resonance with known resonance parameters. The desire to convert experimental upper bounds on T violation into a confidence limit for the strength of the T-violating part of the Hamiltonian, led us to calculate the probability distribution of the relevant ergodic observable δ_T. While the analytical calculation was necessarily approximate, Monte Carlo simulation showed that the analytical result was sufficiently precise to lead to reliable confidence limits. More precisely, the distribution P_a of Eq. (43) will give good, *albeit* somewhat optimistic, estimates of confidence intervals, while

conservative estimates can be obtained using P_c of Eq. (48). A case of even greater complexity would be encountered if the partial width amplitudes of the resonance under observation were unknown themselves. This case can be treated by a slight extension of the procedure of Sec. VI.

In summary, we have established the theoretical framework that is needed to deduce values of or bounds on the symmetry-breaking part of the Hamiltonian from data on isolated CN resonances.

Note added in proof. In a significant recent development, the TRIPLE collaboration has reported on parity-violation data at a number of p-wave resonances in ^{239}U. Independent of the considerations of this paper, the result outlined in Sec. V B 1 was derived and applied to the analysis of the data [J. D. Bowman *et al.*, Phys. Rev. Lett. **65**, 1192 (1990)].

E.D.D. acknowledges support by National Science Foundation (NSF) Grant PHY-87-23182 and discussion with C.R. Gould on experimental details.

APPENDIX A

For the benefit of readers who are not familiar with the formalism of nuclear resonance reactions, we summarize here the formulas for the scattering matrix needed to obtain Eqs. (6), (8), (11), (17), (19), and (26).

Adopting a notation which is slightly more general than in the main body of the paper, we use Latin labels $a,b,c,\ldots$ to denote the channels. (The labels $a,b,\ldots$ include an index to denote the type of two-body fragmentation, the state of excitation of either fragment, as well as the orbital angular momentum of relative motion and the spin couplings. We confine ourselves, however, to a single value J of the total spin of the system.) The quasibound states giving rise to CN resonances are labeled $\mu,\nu,\ldots$, each such index running from 1 to $N \gg 1$. With δ_a denoting the elastic scattering phase shift in channel a, the element $S_{ab}(E)$ of the scattering matrix, taken at energy E, can be written as

$$S_{ab}(E)=e^{i\phi_a}\left\{\delta_{ab}-2\pi i\sum_{\mu\nu}W_{a\mu}[G^{-1}(E)]_{\mu\nu}W_{\nu b}\right\}e^{i\phi_b}\ . \tag{A1}$$

The real amplitudes $W_{a\mu}$ denote coupling matrix elements between channel a and level μ. These amplitudes depend on E; on a scale given by the mean spacing of the CN resonances, this dependence is so weak as to be negligible. The matrix $G_{\mu\nu}$ has the form

$$G_{\mu\nu}(E)=E\delta_{\mu\nu}-H_{\mu\nu}+i\pi\sum_{c\ \text{open}}W_{\mu c}W_{c\nu}\ , \tag{A2}$$

where $H_{\mu\nu}$ are the elements of the Hamiltonian matrix in the space of CN levels, and where a principal value integral involving the $W_{a\mu}$'s has been suppressed. (This is consistent with taking the $W_{a\mu}$ independent of E.) Equations (A1) and (A2) summarize the form of $S_{ab}(E)$ obtained in any of the standard theories of nuclear resonance reactions. To interpret Eqs. (A1) and (A2), it is useful to consider the case $N=1$ for which $S_{ab}(E)$ reduces to the one-level Breit-Wigner form. The form in Eqs. (A1) and (A2) of $S_{ab}(E)$ may be looked upon as the N-level unitary generalization of the Breit-Wigner formula. The most general such form would contain a nondiagonal background term instead of the expression $\delta_{ab}\exp(2i\delta_a)$. We have not considered this case in order to keep the presentation simple.

To describe symmetry-breaking CN reactions, we write the Hamiltonian matrix $H_{\mu\nu}$ in the form of Eq. (10), observing the specifications given below that equation. Diagonalization of the GOE matrix (or matrices) contained in $H^{(0)}$ yields the eigenvalues E_k with a spacing distribution typical for the GOE, while the multiplication of the amplitudes $W_{a\mu}$ with the diagonalizing orthogonal matrix yields the Gaussian distributed amplitudes γ^J_{nj} appearing in the text. Expanding S_{ab} to first order in $H^{(1)}$ and specializing to the one-level or multilevel situation leads to Eqs. (6), (8), (11), (17), (19), and (26).

APPENDIX B

In the absence of any information on neutron partial widths Γ^p_{nj}, an appropriate dimensionless ergodic variable replacing δ_T of Eq. (34) is

$$\hat{\delta}_T=\sum_{k\neq 0}x_k y_k c_k\ , \tag{B1}$$

where x_k and c_k are as defined in Eq. (33) but

$$y_k=\frac{\gamma^{p_0}_{n\,1/2}\gamma^{p_k}_{n\,3/2}-\gamma^{p_0}_{n+1/3}\gamma^{p_k}_{n\,1/2}}{(\overline{\Gamma^p_{n\,3/2}\Gamma^p_{n+1/2}})^{1/2}}\ , \tag{B2}$$

which has a Laplacean probability density: $\frac{1}{2}\exp(-|y_k)$. Equation (36) is replaced by

$$P(\hat{\delta}_T)=\int dE_1 dE_2\cdots P(E_0,E_1,E_2,\ldots)\times\prod_{j\neq 0}\left[\frac{1}{2|c_j|}\int dx_j\exp\left[-\left|\frac{x_j}{c_j}\right|\right]\right]\times\frac{1}{(2\pi\sum_{k\neq 0}x_k^2)^{1/2}}\exp\left[-\frac{1}{2}\frac{\hat{\delta}_T^2}{\sum_{k\neq 0}x_k^2}\right]\ . \tag{B3}$$

We observe that, if all the c_j were fixed and roughly equal, $\sum_{k\neq 0}x_k^2$ would, to a good degree of approximation, be given by $2\sum_j c_j^2$. (We assume that the sum over k runs over many terms: then a central limit theorem applies, implying $\sum_{k\ 0}x_k^2$ has a narrow Gaussian distribution centered at $2\sum_j c_j^2$.) Hence, the subsequent approximate analysis of $P(\hat{\delta}_T)$ can parallel that of Sec. VI.

*On leave of absence from Leningrad Institute of Nuclear Physics, 188 350 Gatchina, Leningrad District, U.S.S.R.

†Present address: Physics Department, University of Arizona, Tucson, AZ 85721.

[1]V. P. Alfimenkov, Usp. Fiz. Nauk **144**, 361 (1984) [Sov. Phys.—Usp. **27**, 797 (1984)].

[2](a) C. D. Bowman *et al.*, in *Fundamental Symmetries and Nuclear Structure,* edited by J. N. Ginocchio and S. P. Rosen (World-Scientific, Singapore, 1989), p. 1; (b) A. Masaike,/p TRIUMF Report 89-5, 1989, p. 126.

[3]I. S. Shapiro, Usp. Fiz. Nauk **95**, 647 (1968) [Sov. Phys.—Usp. **2**, 582 (1969)].

[4]O. P. Sushkov and V. V. Flambaum, Pis'ma Zh. Eksp. Teor. Fiz. **32**, 377 (1980) [JETP Lett. **32**, 352 (1980)].

[5]E. D. Davis, Phys. Lett. B **226**, 197 (1989).

[6]A. Müller, Ph. D thesis, University of Heidelberg, 1990, (unpublished).

[7]V. E. Bunakov, Phys. Lett. **60**, 2250 (1988).

[8]V. E. Bunakov and V. P. Gudkov, in *Tests of Time-Reversal Invariance in Neutron Physics,* edited by N. Roberson, C. Gould, and J. Bowman (World Scientific, Singapore, 1987), p. 175.

[9]V. E. Bunakov and H. A. Weidenmüller, Phys. Rev. C **39**, 70 (1989).

[10]J. B. French, A. Pandey, and J. Smith, see Ref. 8, p. 80.

[11]D. Boosé, H. L. Harney, and H. A. Weidenmüller, Phys. Rev. Lett. **56**, 2012 (1986), Z. Phys. A **325**, 363 (1986).

[12]E. D. Davis, see Ref. 2(a), p. 52.

[13]E. D. Davis and U. Hartmann (unpublished).

[14]C. R. Gould, D. G. Haase, N. R. Roberson, H. Postma, and J. D. Bowman, Int. J. Mod. Phys. A **5**, 2181 (1990).

[15]A. Bohr and B. Mottelson, *Nuclear Structure* (Benjamin, New York, 1969), Vol. 1.

[16]M. L. Mehta, *Random Matrices* (Academic, New York, 1967), Chap. 5.

[17]P. A. Moldauer, Phys. Rev. B **135**, 642 (1964).

[18]J. B. French, P. A. Mello, and A. Pandey, Phys. Lett. **80**B, 17 (1978).

[19]G. Klein and H. Paetz gen. Schieck, Nucl. Phys. **A219**, 422 (1974).